

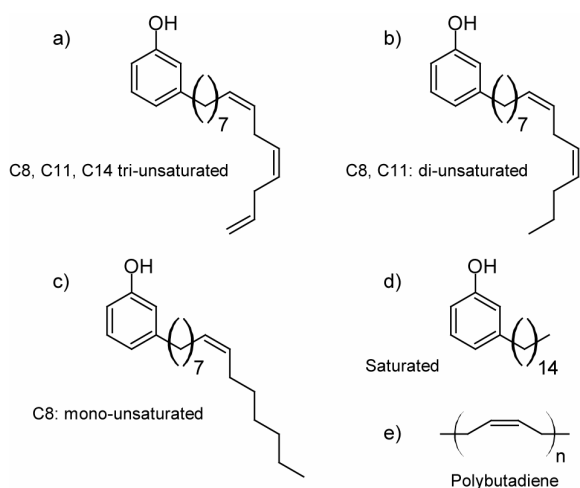
Photoageing of cardanol: characterization, circumvention by side chain methoxylation and application for photocrosslinkable polymers

Thierry Fouquet*, Ludivine Fetzter*, Grégory Mertz, Laura Puchot and Pierre Verge

Luxembourg Institute of Science and Technology (LIST), 5 avenue des Hauts-Fourneaux, 4362
Esch/Alzette (Luxembourg).

Electronic Supplementary Information (ESI)

* To whom correspondence should be addressed:
thierry.fouquet@list.lu, thierry.fouquet83@gmail.com, ludivine.fetzter@list.lu



Scheme S1. Structures of the **a)** tri-unsaturated component 3-(8Z,11Z,14-pentadecatrienyl)-phenol, **b)** di-unsaturated component 3-(8Z,11Z-pentadecadienyl)-phenol, **c)** mono-unsaturated component 3-(8Z-pentadecenyl)-phenol (aka ginkgol 15:1) and **d)** saturated congener 3-(pentadecyl)-phenol constituting the pristine cardanol. **e)** Generic structure of a poly(butadiene).

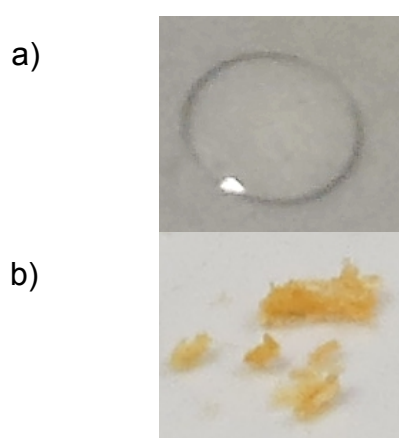


Fig. S1. Photographs of pristine cardanol (light yellow liquid) and 96h photo-aged cardanol (dark yellow wax).

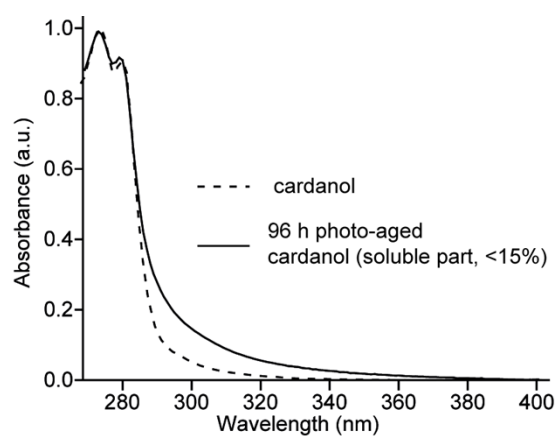


Fig. S2. UV/Vis spectra of **a)** pristine and **b)** 96h photo-aged cardanol solubilized in THF.

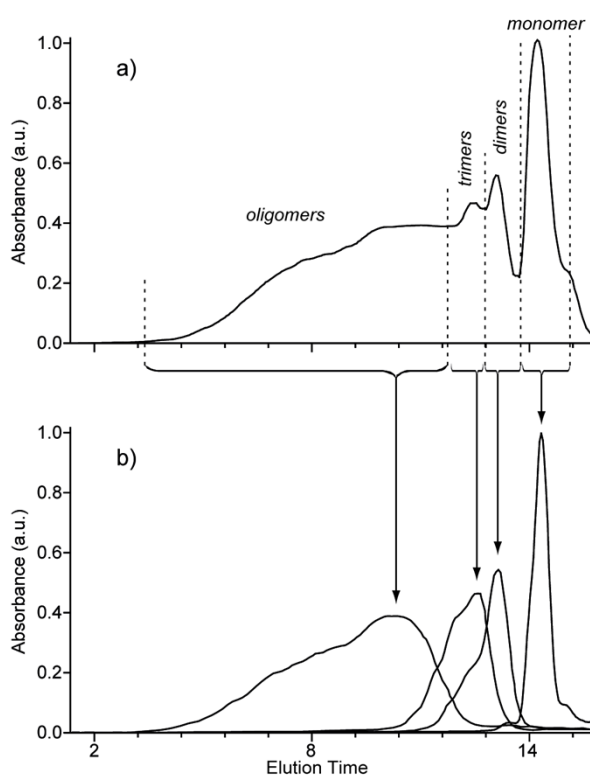


Fig. S3. **a)** SEC chromatogram of a 96h photo-aged cardanol and **b)** SEC chromatograms of the fractions collected from the full SEC chromatogram. Data are recorded from a UV detector set at 280 nm.

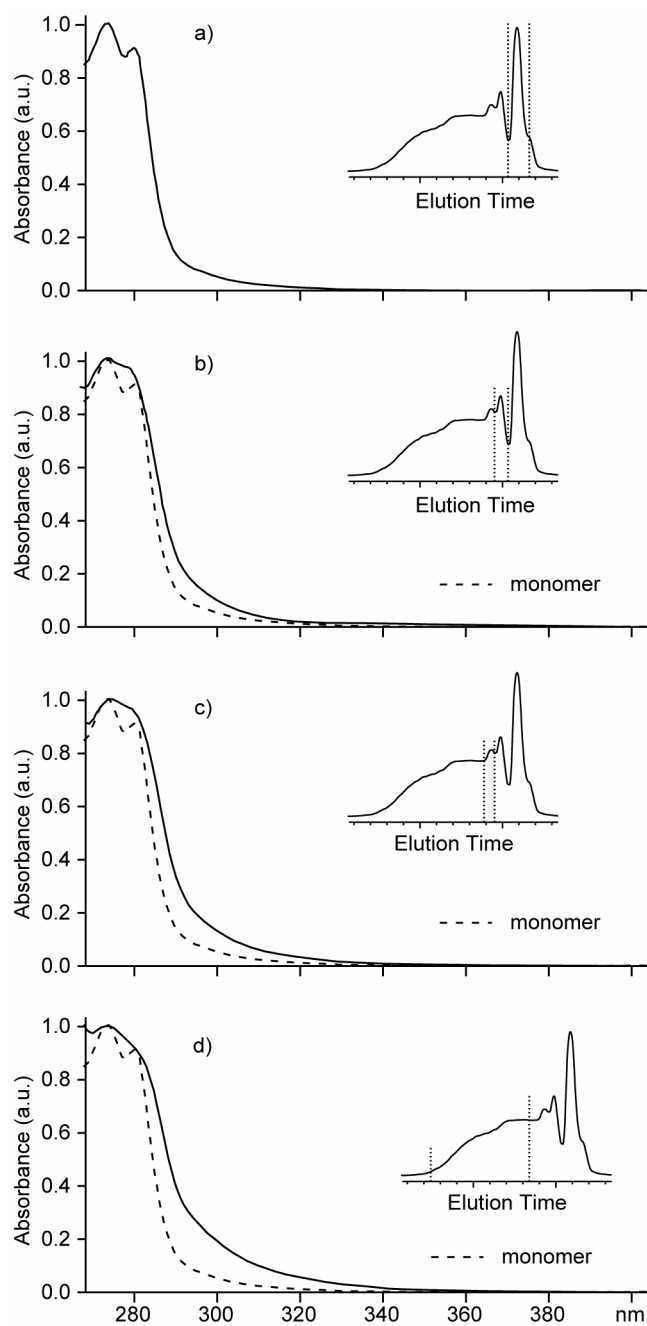


Fig. S4. UV/Vis spectra of **a)** monomers, **b)** dimers, **c)** trimers and **d)** oligomers fractions collected from the SEC elution of a 96h photo-aged cardanol. SEC chromatograms with the fraction of interest are depicted in insets.

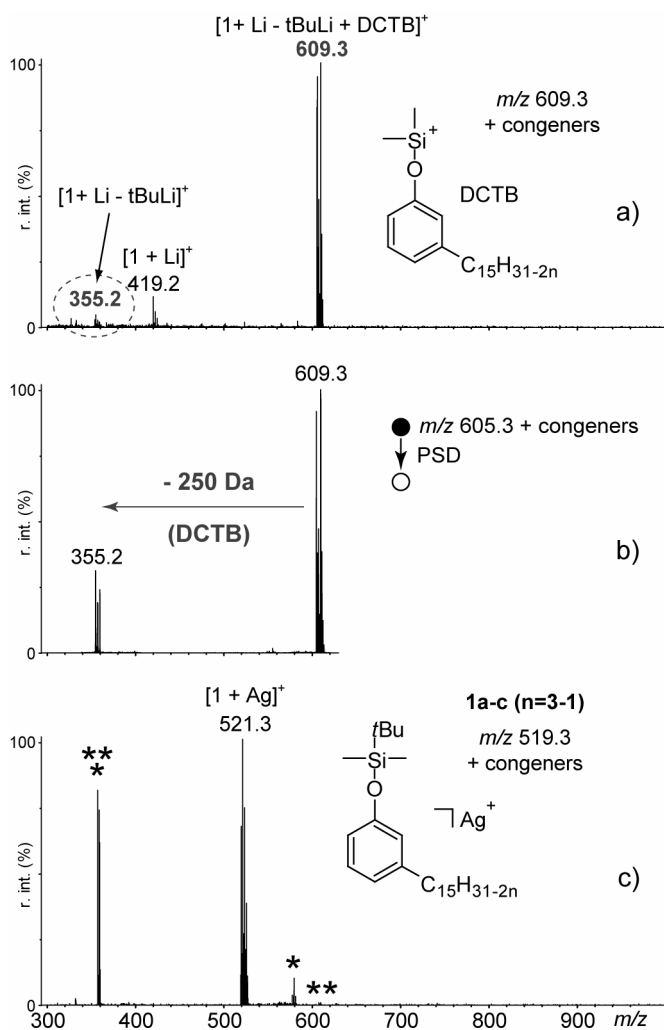


Fig. S5. a) MALDI(+)-MS spectrum of **1** using DCTB and LiTFA. The lithium adduct of TBDMS-cardanol is detected at m/z 419 + congeners. Surprisingly, another ion assigned to a $[1 + \text{Li} - \text{BuLi}]^+$ and especially its DCTB adduct are also found at m/z 355 + congeners and m/z 605 + congeners, respectively. b) PSD-MALDI(+)-MS spectrum of the $[1 + \text{Li} - \text{BuLi} + \text{DCTB}]^+$ adduct at m/z 605 + congeners. c) MALDI(+)-MS spectrum of TBDMS-cardanol using AgTFA as cationizing agent. Silver adduction allows the intact targeted compound **1** (TBDMS-cardanol, $n=3-1$) to be strongly observed. * and ** indicate $[\text{DCTB} + \text{AgTFA} + \text{Ag}]^+$ and $[2^*\text{DCTB} + \text{Ag}]^+$ adducts. *** refers to $[\text{DCTB} + \text{Ag}]^+$.

As discussed for pristine cardanol in the framework of another study [1], DCTB is still observed to form non covalent adducts with a unexpectedly produced $[1 + \text{Li} - \text{BuLi}]^+$ “product” ion from **1**. This butyllithium expulsion remains unexplained at the time of writing, but was observed only when using DCTB as matrix (no neutral loss with 2,5-DHB or TCQN or in SALDI-MS with carbon nanofibers as active surface).

Post Source Decay (PSD) experiments were conducted using the FAST method implemented in FlexControl. The precursor ion was selected using an ion gate with a ± 20 Da selection. The m/z 300 – 650 mass range was analyzed from high to low m/z values in four segments by applying a decreasing reflectron voltage (21 kV for the first segment containing the precursor ion, further lowered to 19.43 kV, 16.80 kV and 13.77 kV). Full PSD-MALDI mass spectra were then recalibrated and overlaid using the FlexAnalysis software.

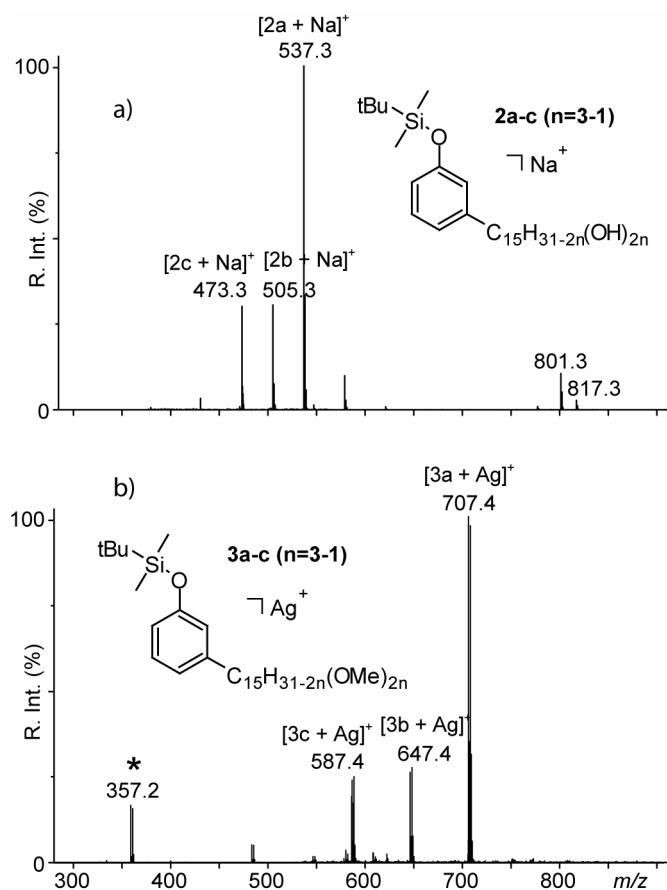


Fig. S6. a) MALDI-MS spectrum of **2** using DCTB and NaTFA. **2c** (mono-unsaturated congener, $n=1$) at m/z 473, **2b** (di-unsaturated congener, $n=2$) at m/z 505 and **2a** (tri-unsaturated congener, $n=3$) at m/z 537 are readily detected. Peaks at m/z 801 and m/z 817 arise from hydroquinine 1,4-phthalazinediyl diether (DHQ)₂PHAL found in the AD-mix alpha catalyst (sodium and potassium adducts, resp.). **b)** MALDI-MS spectrum of **3** using DCTB and AgTFA. Dimethoxylated (**3c**, $n=1$), tetramethoxylated (**3b**, $n=2$) and hexamethoxylated (**3a**, $n=3$) cardanol are found at m/z 567 (+ isotope), m/z 647 (+ isotope) and m/z 707 (+ isotope). * refers to $[DCTB+Ag]^+$.

Incidentally, hydroxylation and subsequent methoxylation of the C15 side chain leads to a *degeneracy of the unsaturation pattern* constituting the pristine cardanol. While forming a narrow pattern with peaks spaced by ± 2 Da in pristine cardanol (**Fig. 4** & **Fig. S5**), with m/z $n=3 < m/z$ $n=2 < m/z$ $n=1$, hydroxylated and methoxylated cardanol exhibit instead three *distinct* peaks spaced by 32 Da and 60 Da, with an inversion of the m/z order: m/z $n=1$ (two OH/OMe) $< m/z$ $n=2$ (four OH/OMe) $< m/z$ $n=3$ (six OH/OMe).

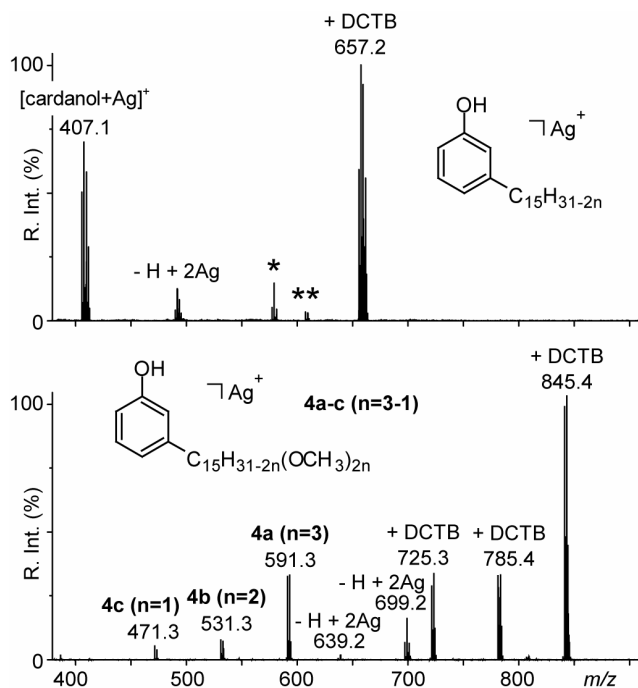


Fig. S7. MALDI-MS spectrum of **a)** pristine cardanol and **b)** methoxylated cardanol **4** recorded in the positive ion mode using DCTB and AgTFA. Pristine cardanol is observed as silver adduct at m/z 407 (+ congeners and isotopes) in **Fig. S7a** while the targeted methoxylated constituents of cardanol are ultimately detected at m/z 471 (+ isotope, **4c**, $n=1$), m/z 531 (+ isotope, **4b**, $n=2$) and m/z 591 (+ isotope, **4a**, $n=3$).

DCTB readily form non covalent adducts with cardanol (m/z 657 + congeners and isotopes in **Fig S7a**). This propensity for adduction is also highlighted here for the methoxylated derivatives, with DCTB adducts detected at m/z 725 (+ isotope), m/z 785 (+ isotope) and m/z 845 (+ isotope) assigned as **4c**, **4b** and **4a** components (**Fig. S7b**). Additional peaks assigned as $[M-H+2Ag]^+$ adducts are also slightly observed for both pristine cardanol (at m/z 513 + congeners and isotopes in **Fig. 7a**) and methoxylated cardanol (m/z 639, **4b**, $n=2$ and m/z 699, **4a**, $n=3$ in **Fig. S7b**).

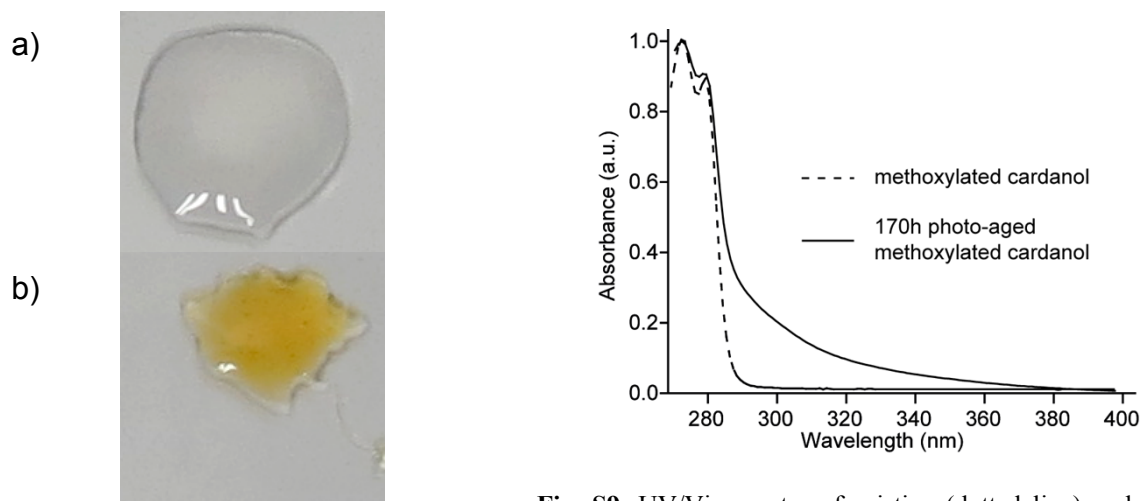


Fig. S8. photographs of **a)** pristine and **b)** 170h aged methoxylated cardanol (fully soluble).

Fig. S9. UV/Vis spectra of pristine (dotted line) and 170h photo-aged cardanol (solid line) solubilized in THF.

A yellowing also occurs under photo-ageing in addition to the increase of the viscosity. The sample remains nevertheless fully soluble. A dimerization process as evidenced by SEC accounts for all these observations. The methoxylation thus avoids a polymerization / crosslinking process to occur, and make this cardanol derivative more resistant towards UV irradiation.

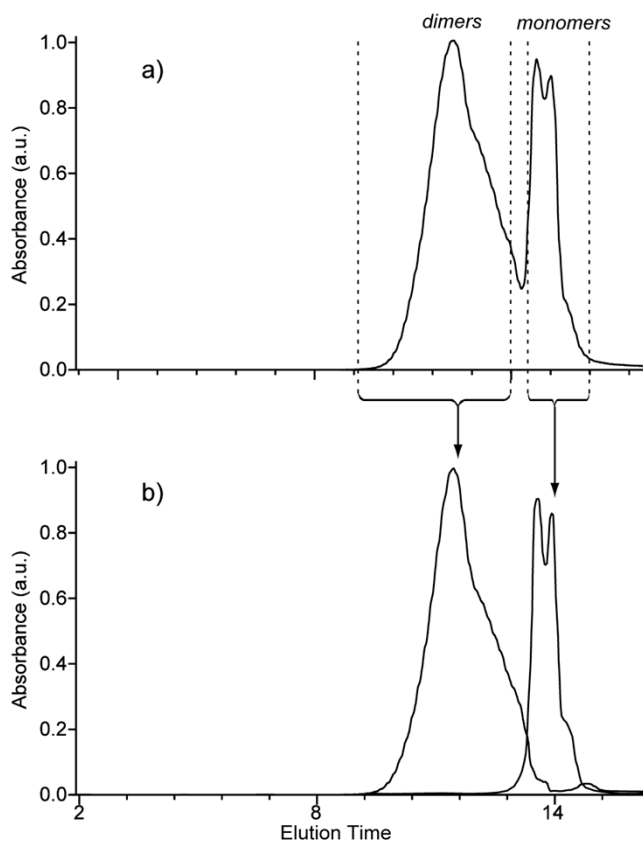


Fig. S10. a) SEC chromatogram of 170h photo-aged methoxylated cardanol **4** and b) SEC chromatograms of the fractions collected from the full SEC chromatogram. Data were recorded from a UV detector set at 280 nm.

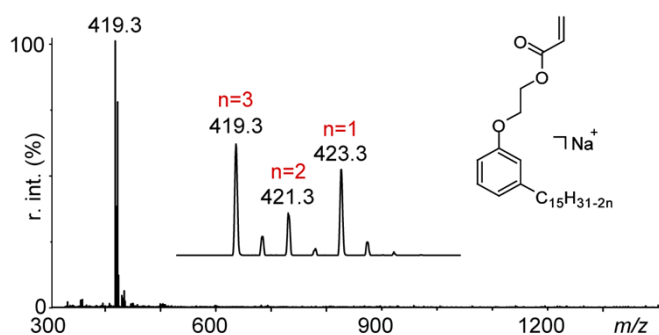


Fig. S11. MALDI(+)-MS spectrum of **8** using DCTB and NaTFA. Structure of the targeted species is depicted in inset.

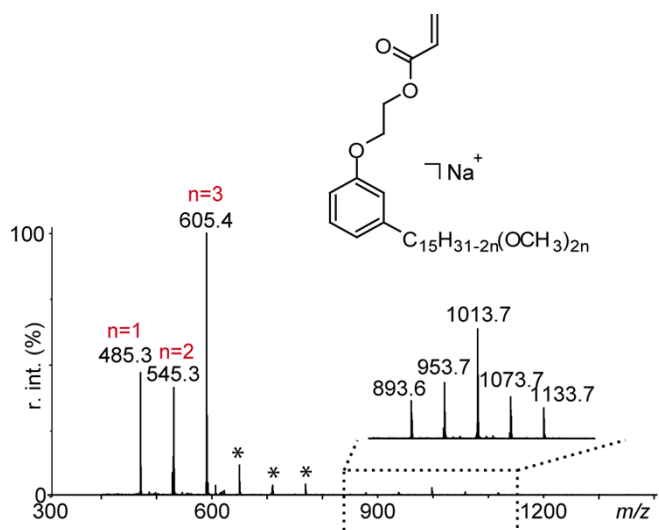
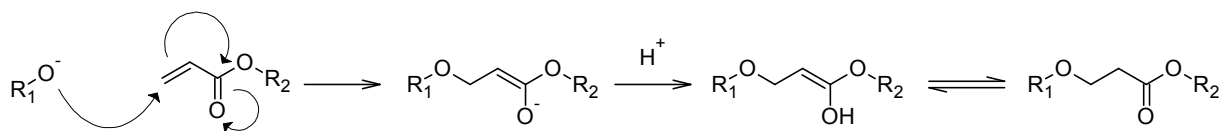


Fig. S12. MALDI(+)-MS spectrum of **12** using DCTB and NaTFA. The structure of the targeted species is depicted in inset. Unexpected dimers are detected in the upper mass range. A hypothetical pathway accounting for the formation upon a side reaction between alkoxides and acrylated species is proposed in **Scheme S2**. Those side-products do not contain the acrylate group anymore and would thus not be incorporated in the copolymer made by ATRP. Their production remains thus anecdotal.



Scheme S2. Hypothetic mechanism of the reaction between alkoxide and the acrylated species accounting for the production of dimers. R_1 and R_2 designate the hydroxyethyl cardanol moieties.

A digression: commercially available hydroxyethyl cardanol as starting reagent

Cardoxyethanol **7** (or hydroxyethyl cardanol) is also commercially available, sold under the references NX9001 and NX9001-LV (for Low Viscosity) by Cardolite Inc. Their use in the synthesis of the acrylate derivatives proposed in **Scheme 2a** (in the main article) would allow one step to be avoided. However, these industrial grades contain a large amount of either oligomers or not fully hydroxyethyl capped cardanol moieties (**Fig. S13**).

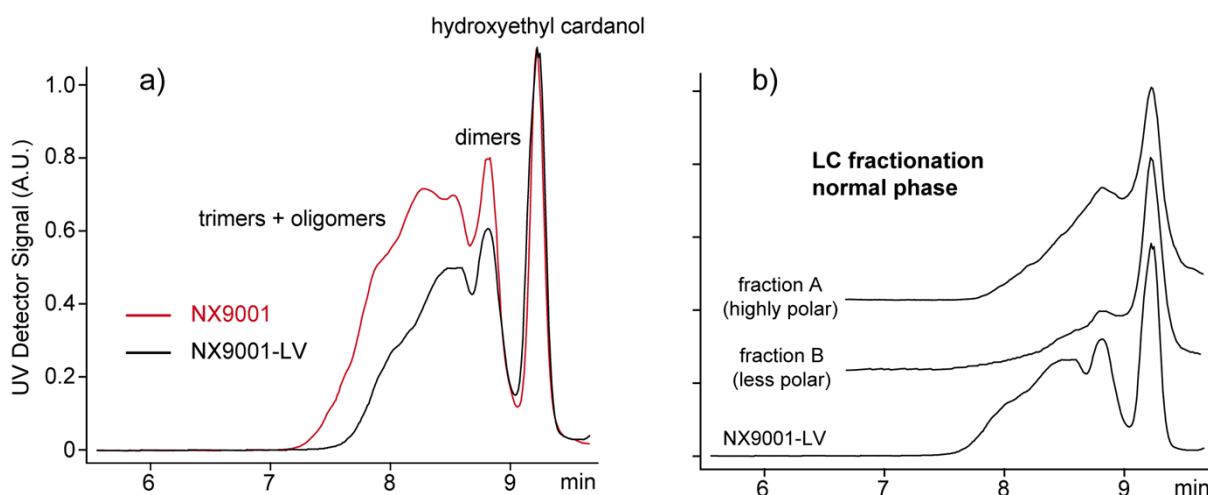


Fig. S13. SEC chromatograms of **a**) cardanol-based “polyols” NX9001 and its “low viscosity” version NX9001-LV and **b**) two fractions collected from a normal phase LC fractionation of NX9001-LV. Elutions were conducted in chloroform and signals recorded from a UV-Vis detector set at a $\lambda=280$ nm.

A normal phase LC fractionation of NX9001-LV allows several fractions to be collected, from the apolar to the most polar ones. SEC chromatograms of the two main fractions exhibit a satisfactory decrease of the content of oligomeric species, especially for the apolar fraction (noted B). These fractions have been further mass analyzed by SEC-MALDI-MS (**Fig. S14**), hence constituting a LC-SEC-MALDI-MS off line coupling.

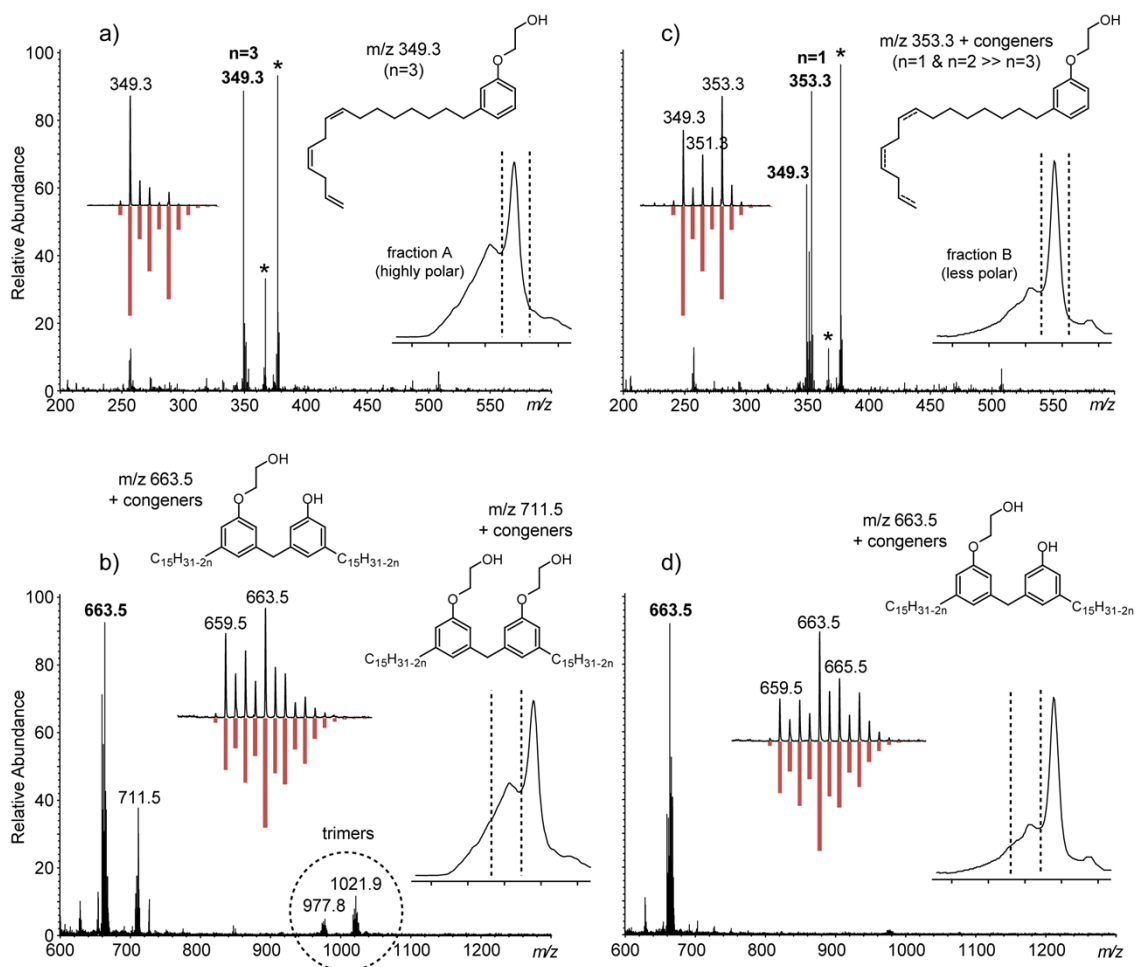


Fig. S14. MALDI-MS spectra from the LC and SEC fractionation of NX9001-LV: fraction **A** (polar) recorded in the **a)** m/z 200-600 and **b)** m/z 600-1300 mass ranges and fraction **B** (apolar) recorded in the **c)** m/z 200-600 and **d)** m/z 600-1300 mass ranges (positive ion mode, DCTB and LiTFA). In insets are depicted the structures of the main compounds, the SEC chromatograms with the collected fraction, as well as the detected unsaturation patterns (up) compared to the simulated patterns (bottom). See [1] for the simulation procedure.

If LC fractionation allows the largest oligomers to be removed, it also clearly induces a discrimination regarding the C15 polyunsaturated side chain(s). While a unique tri-unsaturated cardanol hydroxyethyl ether is observed in fraction **A** (**Fig. S14a**), the three tri-unsaturated, di-unsaturated and mono-unsaturated components are readily detected in fraction **B**, with a slightly reversed relative abundance compared to the (simulated) native product: mono-unsaturated chain appears now as the major constituent. A similar trend is found for the dimeric species: the most unsaturated species are over-detected compared to simulation in fraction **a** and underestimated in fraction **B** (Insets in **Fig. S14b&d**). The polar fraction **A** is also found to contain a non negligible content of dimeric and trimeric species (in accordance with its SEC chromatogram, **Fig. S13b**) while the apolar fraction **B** exhibit one incompletely capped dimer only. One should thus choose Fraction **B** for the reaction pathways described in **Scheme 2**. However, the “abnormal” unsaturation pattern and the presence of residual dimers would lead to unknown molar ratios and purification steps to be added throughout the synthesis route.

[1] T. Fouquet, L. Puchot, P. Verge, J.A.S. Bomfim, D. Ruch, Exploration of cardanol-based phenolated and epoxidized resins by SEC and MALDI-MS, *Analytica Chimica Acta* **2014**, 843, 46.